Secondary electron yield of multiwalled carbon nanotubes

M. K. Alam, P. Yaghoobi, M. Chang, and A. Nojeh[a)]
Department of Electrical and Computer Engineering, University of British Columbia, Vancouver BC V6T 1Z4, Canada

(Received 2 September 2010; accepted 8 December 2010; published online 28 December 2010)

Secondary electron yield from individual multiwalled carbon nanotubes is investigated for a wide range of primary beam energies (0.5–15 keV). By using a simple experimental procedure under an optical microscope, we make suspended nanotubes, which are free from interaction with the substrate during electron yield measurements. It is found that the secondary electron yield from isolated suspended nanotubes is less than unity and decreases as a function of primary electron energy. © *2010 American Institute of Physics*. [doi:10.1063/1.3532851]

Secondary electron (SE) emission from solids has been studied for a long time to understand the fundamentals of the interaction mechanisms with electron beams as well as to make vacuum electronic devices.[1–3] The interaction of electron beams with carbon nanotubes (CNTs) has also been a topic of interest in recent years because of nanotubes' interesting electrical properties and potential for various applications. Nanotubes are hollow cylindrical structures of carbon with nanoscale diameters. The interaction of nanotubes with electron beams and their imaging mechanisms in electron microscopy are expected to be quite different than those of bulk materials. Different imaging mechanisms for CNTs (Refs. 4–8) and high electron yield from coated multiwalled nanotube (MWNT) forests have been reported.[9–11] Energy loss spectra have been calculated for a single nanotube by considering the polarizability of the carbon atoms.[12] SE emission from CNTs has also been studied using first-principles simulations.[13,14]

Recently, Luo *et al.*[15] reported ultrahigh secondary electron gain from the sidewall of single-walled CNTs lying on a dielectric surface. However, the apparent high gain seems to be an artifact of the measurement setup and analysis used: Secondary electrons originating from a large area of the substrate around the nanotube appear to be counted as being from the nanotube. In the present work, we followed a simple procedure to make suspended MWNTs and a widely used experimental method of measuring electron yield to calculate the intrinsic SE yield of individual CNTs, free from interaction with the substrate. We found that the true SE yield of individual MWNTs is less than unity for a wide range of primary electron energies.

We used nanotubes grown using chemical vapor deposition. The fabrication procedure has been described elsewhere in detail.[16] Briefly, microfabrication was used for patterning catalyst (10 nm of Al and 2 nm of Fe), and ethylene was used as the carbon source to grow vertically aligned millimeter-long forests (collections of individual CNTs) of MWNTs on a highly doped silicon substrate [Fig. 1(b)].

Traditionally, SEs are defined as those leaving the sample with an energy of less than 50 eV. To measure the intrinsic SE yield from CNTs, one needs to isolate the CNTs from the forests and the substrate. We adopted a method of attaching CNTs to sharp conductive tips under an optical microscope that has been mainly used for generating CNT-tips for atomic force microscopy [Fig. 1(a)].[17] For the purposes of our experiments, we performed this procedure with tungsten tips (tip diameter: 0.2–20 μm). Two micromanipulators were used to bring a tip and a forest close to each other, and an electric arc discharge was induced by using an external dc source to attach one or a few suspended CNTs to the tip [Fig. 1(c)].

The tips were then placed in a Hitachi S-570 scanning electron microscope (SEM) for SE yield measurement and connected to a Keithley 6517A electrometer capable of bias-

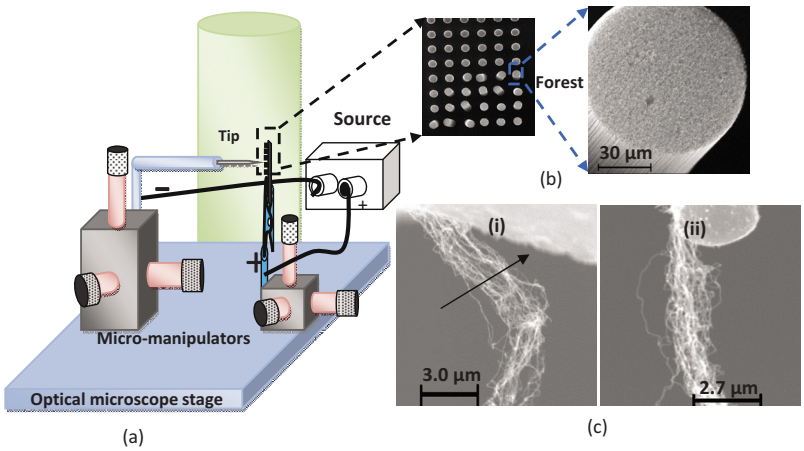

FIG. 1. (Color online) (a) Schematic of the experimental setup for extracting CNTs from the forests, (b) micrograph of the CNT forests, and (c) extracted CNTs on tungsten tips.

[a)]Author to whom correspondence should be addressed. Electronic mail: anojeh@ece.ubc.ca.

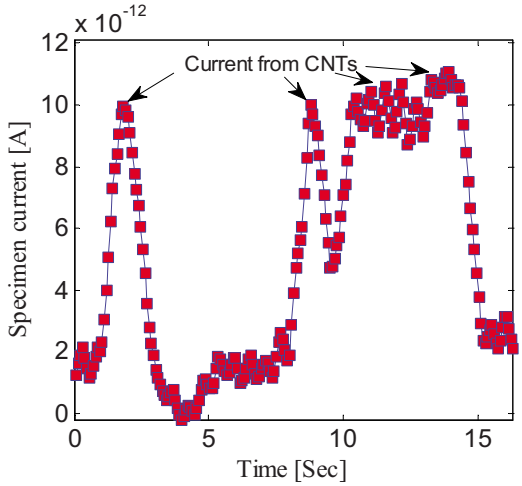

FIG. 2. (Color online) Specimen current at 1 keV as the beam was moved across the CNTs [along the arrow indicated in Fig. 1(c)].

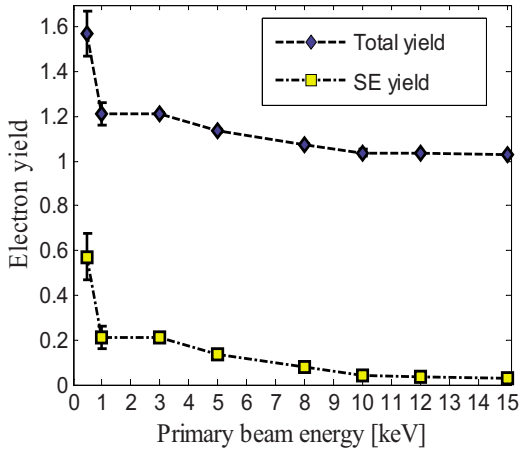

FIG. 3. (Color online) Electron yield measured from the suspended CNTs (total yield, diamond marker and SE yield, square marker). Fluctuations in the beam current or specimen current are included in error bars.

ing the specimen and measuring currents with femtoampere accuracy. The measurement procedure has been described in our previous work on the SE yield measurement from CNT forests.[16] We used the same experimental configuration with an extra Faraday cup (grounded) under the suspended nanotubes to block backscattered or secondary electrons from the surface underneath the device (due to the small and hollow CNT structure, most of the "backscattered" electrons are, in fact, scattered with a small scattering angle and collected in the Faraday cup, making SE generation from the chamber walls negligible). The small size of the specimen further reduces the probability of being hit by SEs generated from the surrounding walls.[16] Another Faraday cup was used for primary current measurements. As the individual CNTs are hollow and made of a single/a few layer(s) of carbon [with interwall distance of ~0.34 nm for MWNTs (Ref. 18)], electron energy loss in them is expected to be extremely small and the primary electrons are expected to leave the CNT with an energy far greater than 50 eV, thus effectively being counted as "backscattered" electrons. In other words, no high-energy electron is captured by the CNT and the backscattered yield for suspended CNTs is unity. We measured the total yield from the CNTs while applying −50 V to the specimen (to ensure that all electrons, including secondaries, escape the sample). We then subtracted the backscattered yield (unity) to calculate the true SE yield[16]

$$\text{total yield} = \frac{\text{total emitted current}}{\text{primary current}}, \tag{1}$$

$$\text{SE yield} = \text{total yield} - \text{backscattered yield}. \tag{2}$$

We performed the experiments on samples with a few individual CNTs. The beam was slowly moved along a line [black arrow in Fig. 1(c)] across the CNTs in the spot mode, and the specimen current was recorded (Fig. 2). The electrometer interfaced with a PC was used for real-time data acquisition. A running average was used for current measurements to reduce noise and fluctuations (analog-to-digital converter integration time: 16.67 ms, moving averaging: 10 points, and median filtering: 3 points). A peak in Fig. 2 indicates that the beam is crossing a CNT.

Figure 3 shows the total and the SE yield calculated from Eqs. (1) and (2). As can be seen, the SE yield from individual CNTs is less than unity and decreases as a function of energy for the measured energy range. The experiment was repeated on another specimen [Fig. 1(c)(ii)] at several primary energies, and similar values of electron yield were obtained. The low yield from individual CNTs can be attributed to the very weak stopping power (corresponding to small energy loss of the primary electron) of the CNT. A high-energy electron cannot lose a significant amount of energy through inelastic collisions because of the hollowness, small dimension, and thin atomic wall of the CNT. Also, it is very unlikely for the primary electron to go through multiple scattering processes given that the mean free path is expected to be much higher than the thickness of the CNT sidewalls.[3,19] It has been predicted using first-principles calculations that the molecular orbitals of the nanotube can be raised in energy due to the presence of an external electron beam, thus effectively reducing the workfunction. This can help in emitting SEs and making the CNTs visible in a SEM.[14] Nonetheless, a small SE yield is obtained (unless a strong external field is also applied and electron-stimulated field-emission occurs[20]). The decreasing trend of the electron yield is because of the decrease in energy loss of the primary electron with the increase in the beam energy.[14] We used the modified Bethe equation provided by Joy and Luo[21] to calculate the energy loss in a single CNT (the Bethe energy loss formula has previously been used to calculate the average energy transfer through a single inelastic scattering in CNT bundles[22]). We then used the following parametric equation to calculate the SE yield:[3]

$$\delta = A\frac{1}{\varepsilon}\int_a^b \frac{dE}{dz} \times p(z)dz. \tag{3}$$

Here ε is an empirical parameter corresponding to the average energy needed for SE generation, dE/dz is the energy loss rate, and $p(z)$ is the escape probability (for solids, an exponential function of the depth). A is an empirical parameter, representing the percentage of the electrons emitted toward the outside of the material. Since SEs can escape from any side of a suspended CNT, the empirical constant A can be taken as 1 for our case. Also, given the hollow nanotube structure with a sidewall thickness smaller than the typical escape depth in solids, the escape probability can be assumed to be approximately 100%. The value of ε for carbon has

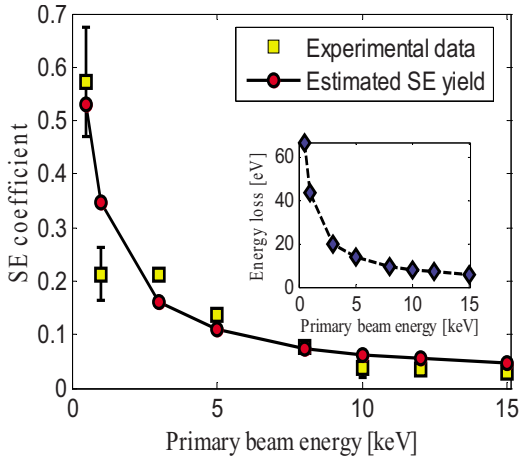

FIG. 4. (Color online) Comparison of the experimental data with the theoretically estimated SE yield. The inset shows the behavior of electron energy loss.

been reported to be 125 eV.[3] Using this value of ε, an interaction length [integration range, $b-a$, in Eq. (3)] of 2 nm gives a reasonable fit to the experimental data (Fig. 4). The predicted value of a few nanometers for the interaction length correlates well with the sidewall thickness of our nanotubes, as observed using transmission electron microscopy.[16] For instance, a four-wall MWNT has a total sidewall thickness of ~ 2 nm.

Note that the interaction length would vary with the chiralities and number of walls in MWNTs and may not be exactly equal to the thickness of the CNT wall. Nevertheless, it is expected to be in the order of the wall thickness, and the trend of the SE yield as a function of primary energy will not be affected by small changes in the interaction length; only an upward or downward shift of the curve will be seen with the change in this or in other empirical parameters. Therefore, our measured data follow a trend consistent with the predictions of established models for bulk solids.

It should also be noted that a CNT tends to be positively charged under electron irradiation as it loses electrons and hardly captures any primary electron. However, if the CNT is connected to an external source (the present case), there should not be significant charging as the lost electrons are supplied from the biasing source. If the nanotubes are electrically isolated, they would soon become positively charged to the point of preventing further secondary emission. In general, charging effects play an important role in the imaging of CNTs. For example, if there is a substrate under a charged suspended CNT, the charge distribution on the surface of the substrate below the CNT could change and, therefore, the SE yield of the substrate at that location could also change, or the charged nanotube could deflect the secondaries emitted by the substrate underneath.[6] If the CNT lies on a surface, depending on its potential relative to the substrate, it could increase or decrease the SE emission from the substrate in its immediate surroundings.[4]

In summary, SE yield from isolated suspended multiwalled CNTs was measured systematically and a low yield was obtained. The method can also be used for single-walled CNTs. These results have important implications on our understanding of the interaction of electron beams with CNTs. The data may also be used in Monte-Carlo simulations of structures made of collections of CNTs (with or without other materials) to predict their electron yield for potential device applications. The results can also assist in finding the optimum imaging conditions of nanotube-based devices in electron microscopy to control artifacts such as charging.

We acknowledge financial support from the Natural Sciences and Engineering Research Council (NSERC Grant Nos. 341629-07 and 361503-09), the Canada Foundation for Innovation (CFI Grant No. 13271), the British Columbia Knowledge Development Fund (BCKDF), the BCFRST foundation, and the British Columbia Innovation Council (BCIC). M.K.A. and P.Y. also thank the University of British Columbia for additional support.

[1] K. G. McKay, *Secondary Electron Emission: Recent Advances in Electronics* (Academic, New York, 1948).
[2] L. Reimer, *Scanning Electron Microscopy: Physics of Image Formation and Microanalysis* (Springer, Berlin, 1998).
[3] D. C. Joy, *Monte Carlo Modeling for Electron Microscopy and Microanalysis* (Oxford University Press, New York, 1995).
[4] T. Brintlinger, Y.-F. Chen, T. Dürkop, E. Cobas, M. S. Fuhrer, J. D. Barry, and J. Melngailis, Appl. Phys. Lett. **81**, 2454 (2002).
[5] A. Nojeh, W.-K. Wong, A. W. Baum, R. F. W. Pease, and H. Dai, Appl. Phys. Lett. **85**, 112 (2004).
[6] P. Finnie, K. Kaminska, Y. Homma, D. G. Austing, and J. Lefebvre, Nanotechnology **19**, 335202 (2008).
[7] Y. Homma, S. Suzuki, Y. Kobayashi, M. Nagase, and D. Takagi, Appl. Phys. Lett. **84**, 1750 (2004).
[8] W. K. Wong, A. Nojeh, and R. F. W. Pease, Scanning **28**, 219 (2006).
[9] W. Yi, S. Yu, W. Lee, I. T. Han, T. Jeong, Y. Woo, J. Lee, S. Jin, W. Choi, J. Heo, D. Jeon, and J. M. Kim, J. Appl. Phys. **89**, 4091 (2001).
[10] W. S. Kim, W. Yi, S. Yu, J. Heo, T. Jeong, J. Lee, C. S. Lee, J. M. Kim, H. J. Jeong, Y. M. Shin, and Y. H. Lee, Appl. Phys. Lett. **81**, 1098 (2002).
[11] J. Lee, J. Park, K. Sim, and W. Yi, J. Vac. Sci. Technol. B **27**, 626 (2009).
[12] A. Rivacoba and F. J. García de Abajo, Phys. Rev. B **67**, 085414 (2003).
[13] A. Nojeh, B. Shan, K. Cho, and R. F. W. Pease, Phys. Rev. Lett. **96**, 056802 (2006).
[14] M. K. Alam, S. P. Eslami, and A. Nojeh, Physica E **42**, 124 (2009).
[15] J. Luo, J. H. Warner, C. Feng, Y. Yao, Z. Jin, H. Wang, C. Pan, S. Wang, L. Yang, Y. Li, J. Zhang, A. A. R. Watt, L. M. Peng, J. Zhu, and G. A. D. Briggs, Appl. Phys. Lett. **96**, 213113 (2010).
[16] M. K. Alam, P. Yaghoobi, and A. Nojeh, Scanning **31**, 221 (2009).
[17] R. M. D. Stevens, N. A. Frederick, B. L. Smith, D. E. Morse, G. D. Stucky, and P. K. Hansma, Nanotechnology **11**, 301 (2000).
[18] X. Liang, Z. Fu, and S. Y. Chou, Nano Lett. **7**, 3840 (2007).
[19] I. Kyriakou, D. Emfietzoglou, R. Garcia-Molina, I. Abril, and K. Kostarelos, Appl. Phys. Lett. **94**, 263113 (2009).
[20] J. M. Michan, P. Yaghoobi, B. Wong, and A. Nojeh, Phys. Rev. B **81**, 195438 (2010).
[21] D. C. Joy and S. Luo, Scanning **11**, 176 (1989).
[22] D. Emfietzoglou, I. Kyriakou, R. Garcia-Molina, I. Abril, and K. Kostarelos, J. Appl. Phys. **108**, 054312 (2010).